# Expanding the Crystal Chemistry of Uranyl Peroxides: Four Hybrid Uranyl-Peroxide Structures Containing EDTA

Jie Qiu,[†] Jie Ling,[†] Claire Sieradzki,[†] Kevin Nguyen,[‡] Ernest M. Wylie,[†] Jennifer E. S. Szymanowski,[†] and Peter C. Burns*,[†,‡]

[†]Department of Civil and Environmental Engineering and Earth Sciences and [‡]Department of Chemistry and Biochemistry, University of Notre Dame, Notre Dame, Indiana 46556, United States

Ⓢ *Supporting Information*

ABSTRACT: The first four uranyl peroxide compounds containing ethylenediaminetetra-acetate (EDTA) were synthesized and characterized from aqueous uranyl peroxide nitrate solutions with a pH range of 5−7. Raman spectra demonstrated that reaction solutions that crystallized $[NaK_{15}[(UO_2)_8(O_2)_8(C_{10}H_{12}O_{10}N_2)_2(C_2O_4)_4]\cdot(H_2O)_{14}]$ (**1**) and $[Li_4K_6[(UO_2)_8(O_2)_6(C_{10}H_{12}O_{10}N_2)_2(NO_3)_6]\cdot(H_2O)_{26}]$ (**2**) contained excess peroxide, and their structures contained oxidized ethylenediaminetetraacetate, $EDTAO_2^{4-}$. The solutions from which $[K_4[(UO_2)_4(O_2)_2(C_{10}H_{13}O_8N_2)_2(IO_3)_2]\cdot(H_2O)_{16}]$ (**3**) and $LiK_3[(UO_2)_4(O_2)_2(C_{10}H_{12}O_8N_2)_2(H_2O)_2]\cdot(H_2O)_{18}$ (**4**) crystallized contained no free peroxide, and the structures incorporated intact $EDTA^{4-}$. In contrast to the large family of uranyl peroxide cage clusters, coordination of uranyl peroxide units in **1−4** by $EDTA^{4-}$ or $EDTAO_2^{4-}$ results in isolated tetramers or dimers of uranyl ions that are bridged by bidentate peroxide groups. Two tetramers are bridged by $EDTAO_2^{4-}$ to form octamers in **1** and **2**, and dimers of uranyl polyhedra are linked through iodate groups in **3** and $EDTA^{4-}$ in **4**, forming chains in both cases. In each structure the U−O$_2$−U dihedral angle is strongly bent, at ∼140°, consistent with the configuration of this linkage in cage clusters and other recently reported uranyl peroxides.
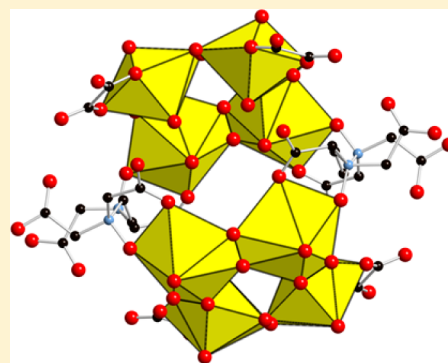
INTRODUCTION

The peroxide group has a strong affinity for uranyl ions that far exceeds that of other inorganic ligands including fluoride, hydroxyl, carbonate, nitrate, and water.[1] This affinity is significant in various aspects of the nuclear fuel cycle, including in the mining and purification of uranium and potentially in the reprocessing of used nuclear fuels.[2] Uranyl peroxide solids can be remarkably stable, with the minerals studtite, $(UO_2)(O_2)(H_2O)_2(H_2O)_2$, and its lower hydrate, metastudtite, $(UO_2)(O_2)(H_2O)_2$, forming and persisting in natural U deposits due to the buildup of peroxide owing to the alpha radiolysis of water.[3] The synthetic analogues of these minerals are known to form on irradiated nuclear fuel when it interacts with water,[4] as well as on nuclear debris from the Chernobyl accident where it is exposed to the environment.[5] For studtite, the crystal structure,[6] spectra,[7,8] solid morphology,[9] electrochemical activity,[10] stability,[3,11] and sorption capacity for some radionuclides[12−14] have been examined.

Over the past decade a family of complex nanoscale uranyl peroxide cage clusters has been described that consist of as many as 124 uranyl ions.[15−19] These clusters self-assemble in aqueous solution under ambient conditions when uranyl is combined with peroxide and various counterions,[20] and they also exhibit remarkable stability.[21] On the basis of experimental and computational evidence, it has been argued that a partially covalent interaction between the uranyl and peroxo favors a bent configuration in the case where uranyl ions are bridged by

bidentate peroxide and that this bent interaction supports the formation of cage clusters.[22,23] Aside from the cage clusters, several other uranyl peroxide compounds have been reported recently that include $Na_5[(UO_2)_3(O_2)_4(OH)_3](H_2O)_{13}$[24] based on sheets of uranyl peroxide polyhedra; $Na_4[UO_2(O_2)_3]\cdot 9H_2O$,[25] $K_4[UO_2(CO_3)_2(O_2)]\cdot 2.5H_2O$,[26] $Na_4(UO_2)(O_2)_3(H_2O)_{12}$,[27] $Ca_2(UO_2)(O_2)_3(H_2O)_9$,[27] $Na_6[UO_2(O_2)_2(OH)_2]\cdot(OH)_2\cdot 14H_2O$,[28] and $Li_4[UO_2(O_2)_3]\cdot 10H_2O$,[29] with monomers of uranyl peroxide polyhedra; $[HNEt_3]_2[(UO_2)_2L_2O_2(H_2O)_2]\cdot 2H_2O$ (L= pyridine-2,6-dicarboxylate),[30] $Na_2Rb_4(UO_2)_2(O_2)_5(H_2O)_{14}$,[27] $K_6[(UO_2)(O_2)_2(OH)]_2(H_2O)_7$,[27] and $K_6(H_2O)_4[(UO_2)_2(O_2)(C_2O_4)_4]$,[22] containing dimers of uranyl peroxide polyhedra; and $K_2[Mg(H_2O)_6]_4[(UO_2)_3(O_2)_8]\cdot 2H_2O$,[31] $K_{10}[(UO_2)(O_2)(C_2O_4)]_5(H_2O)_{13}$,[22] and $Na_{12}[(UO_2)(O_2)(C_2O_4)]_6(H_2O)_{29}$[22] with trimers, pentamers, and hexamers of uranyl peroxide polyhedra, respectively.

We are especially interested in the structures and stabilities of uranyl peroxides because of their importance in the nuclear fuel cycle, their potential importance in various accident scenarios involving nuclear fuels, such as the core-melt incidents that occurred in Fukushima, Japan, in 2011, or Chernobyl, Ukraine, in 1986, and the remarkable structures exhibited that are a dramatic departure from typical uranyl compounds that are

Table 1. Crystallographic Data and Structure Refinement Results for Compounds 1−4

	1	2	3	4
formula	$C_{28}K_{15}N_4NaO_{82}U_8$	$C_{20}K_6Li_8N_{10}O_{92}U_8$	$C_{20}I_2K_4N_4O_{50}U_4$	$C_{20}K_3N_4O_{48}U_4$
fw	4187.16	4046.66	2458.56	2133.66
space group	$C2/m$	$P\bar{1}$	$C2/c$	$P\bar{1}$
a [Å]	17.426(2)	13.477(3)	34.074(3)	10.5051(11)
b [Å]	20.204(3)	14.799(4)	16.2211(15)	11.1060(12)
c [Å]	14.2568(19)	24.568(6)	28.278(4)	12.3307(13)
α [°]	90	93.156(3)	90	91.9030(10)
β [°]	106.5248(16)	94.272(3)	124.7430(10)	99.0390(10)
γ [°]	90	106.106(3)	90	106.2520(10)
V [Å³]	4812.2(11)	4680(2)	12843(2)	1359.5(2)
Z	2	2	8	1
ρ_{calcd} (g/cm³)	2.890	2.872	2.543	2.606
μ (Mo Kα) (mm⁻¹)	14.15	14.19	11.39	12.23
2θ (min, max) [°]	1.49, 27.47	1.44, 27.27	1.45, 27.13	1.68, 27.47
total reflections	28603	54013	72914	16113
N_{ref}, N_{par}	5654, 167	20665, 663	14187, 387	6160, 173
R_{int}	0.0723	0.0561	0.0788	0.0336
R_1 $(I > 2\sigma(I))$	0.0496	0.0498	0.0495	0.0363
R_1 (all data)	0.0767	0.0784	0.0828	0.0381
wR_2 $(I > 2\sigma(I))$	0.1633	0.1404	0.1464	0.1009
wR_2 (all data)	0.1822	0.1594	0.1717	0.1020
S	1.163	0.972	1.097	1.047

dominated by sheet structural units.[32] Whereas most uranyl minerals are based upon sheets of uranyl polyhedra or combinations of uranyl polyhedra and other polyhedra containing higher-valence cations,[32] uranyl peroxides are dominated by monomers, clusters, and chains of uranyl peroxide polyhedra. In the current study, we examine the interaction of uranyl peroxide polyhedra with ethylenediaminetetraacetate (EDTA), a common synthetic chelating agent that is also a stable contaminant in various surface and groundwaters.[33] EDTA is used in decontamination of reactor components and is present in nuclear waste.[34] It is a flexible diaminopolycarboxylate ligand with 10 potentially coordinating sites (eight O atoms and two N atoms) that has strong chelating ability. EDTA can affect the sorption[35,36] and redox[37,38] behaviors of uranium by forming stable complexes and thus impacts the mobility of uranium in the environment. Only limited crystal structures of these complexes have been isolated,[39,40] although structures of transition metal and lanthanide based complexes containing EDTA have been widely investigated.[41−49] In the current study, the first four uranyl peroxide compounds containing EDTA groups were isolated and characterized from solutions containing hydrogen peroxide over a pH range of 5−7.

■ EXPERIMENTAL SECTION

Synthesis. Caution! Although the isotopically depleted uranium used in this study has a very long half-life, precautions for working with radioactive materials should be followed, and such work should only take place in appropriate facilities and be conducted by properly trained individuals.

All chemicals were purchased as reagent grade and were used to prepare aqueous solutions without further purification. All syntheses reactions were done in 5 mL glass vials under ambient conditions. In each synthesis, yellow crystals grew from solutions with pH in the range of 5−7 during evaporation of the solution in air.

Compound **1** was synthesized by loading solutions containing 0.05 mmol of $UO_2(NO_3)_2·6H_2O$ (0.5 M, 0.1 mL) and 1.0 mmol of H_2O_2 (30% (w/w), 0.1 mL) in a glass vial, resulting in the formation of a

yellow precipitate. Addition of an alkaline solution containing 0.2 mmol of tetraethylammonium hydroxide (TEAH, 40% (W/W), 0.075 mL) increased the pH of the solution and the precipitate dissolved. Solutions containing 0.03 mmol of sodium mesoxalate (0.1 M, 0.3 mL) and 0.1 mmol of EDTA acid dipotassium salt dihydrate ($H_2K_2EDTA·2H_2O$, 0.5 M, 0.2 mL) were added, resulting in a clear solution with a pH of 6.7. Small thin square crystals formed within 2 weeks, together with a fine-grained precipitate. The yield of crystals of **1** was >50% on the basis of uranium. Initially, we sought a compound containing mesoxalate and EDTA. However, the mesoxalate decomposed to give oxalate during the reaction.

We found that the pure potassium salt of complex **1** was readily synthesized directly using oxalic acid. This synthesis was achieved by combining aqueous solutions containing 0.05 mmol of $UO_2(NO_3)_2·$ $6H_2O$ (0.5 M, 0.1 mL), 1.0 mmol of H_2O_2 (30%, 0.1 mL), 0.24 mmol of LiOH (2.4 M, 0.1 mL), 0.015 mmol of oxalic acid ($H_2C_2O_4$, 0.5 M, 0.03 mL), and 0.1 mmol of $H_2K_2EDTA·2H_2O$ (0.5 M, 0.2 mL), giving a clear solution with a pH of 6.1. As in the previous synthesis, small crystals were mixed with a fine-grained precipitate in relatively low yield.

Compound **2** was synthesized by combining aqueous solutions containing 0.05 mmol of $UO_2(NO_3)_2·6H_2O$ (0.5 M, 0.1 mL), 1.0 mmol of H_2O_2 (30% in H_2O, 0.1 mL), and 0.24 mol of LiOH (2.4 M, 0.1 mL), followed by shaking until a clear solution resulted. Solutions containing 0.1 mmol of acetic acid (0.5 M, 0.2 mL) and 0.025 mmol of $H_2K_2EDTA·2H_2O$ (0.5 M, 0.05 mL) were added, resulting in a solution that remained clear with a pH of 5.5. A few tabular crystals formed within one month, together with fine grained precipitate. The yield of crystal was very low.

Compound **3** was synthesized by combining solutions containing 0.05 mmol of $UO_2(NO_3)_2·6H_2O$ (0.5 M, 0.1 mL), 1.0 mmol of H_2O_2 (30%, 0.1 mL), and 0.27 mmol of TEAH (40%, 0.1 mL), and shaking resulted in a clear solution. Subsequently, aqueous solutions containing 0.075 mmol of HIO_3 (0.5 M, 0.15 mL) and 0.15 mmol of $H_2K_2EDTA·2H_2O$ (0.5 M, 0.3 mL) were added, resulting in a clear solution with a pH of 6.1. Block-shaped crystals formed within 2 weeks with a yield of 48% on the basis of uranium.

Compound **4** was synthesized by mixing a solution containing 0.15 mmol of $H_2K_2EDTA·2H_2O$ (0.5 M, 0.3 mL) and 0.3 mL of a solution containing the uranyl peroxide cluster U_{60},[50] giving a solution with a pH of 6.4. Relatively large block crystals of **4** grew within 2 weeks as

the solution slowly evaporated. Cluster U_{60} was synthesized by combining aqueous solutions containing 0.15 mmol of $UO_2(NO_3)_2 \cdot 6H_2O$ (0.5 M, 0.3 mL), 3.0 mmol of H_2O_2 (30%, 0.3 mL), 0.48 mmol of LiOH (2.4 M, 0.2 mL), and 0.03 mmol of KCl (0.3 M, 0.1 mL), giving a solution with a pH of 9.0. Cubic crystals of U_{60} grew from the solution within 2 weeks. Clear solution above the growing crystals was harvested and used for the synthesis of compound **4**. The yield of **4** was 48% on the basis of uranium.

Single Crystal X-ray Diffraction. A single crystal of each compound was mounted on a cryoloop using mineral oil under an optical microscope, and the cryoloop was aligned on the goniometer of a Bruker APEX II Quazar diffractometer, where the crystal was cooled by flowing nitrogen gas at 100 K. The diffractometer was equipped with graphite monochromated Mo Kα X-radiation provided by a conventional sealed tube. The Bruker APEXII software was used for determination of the unit cells and for data collection control. A complete sphere of data was collected for each crystal using frame widths of 0.5° in ω and an exposure time per frame of 40 s. The APEXII software was used for data integration, including corrections of Lorentz, polarization, and background effects. SADABS[51] was used for semiempirical absorption corrections. SHELXTL[52] was used for structure solutions and refinements. Only U, I, and K sites were refined anisotropically; attempts to refine anisotropic displacement parameters for O sites resulted in physically unrealistic parameters in some cases. As is typical for uranyl compounds, the H atoms were not located in the structures. Crystallographic information is summarized in Table 1. CIF files are in the Supporting Information.

Chemical Analysis. *U, K, and Li Analysis.* About 10 mg of crystals for each compound was harvested, vacuum filtered, rinsed using 20 mL of water, and dissolved in 0.5 mL of concentrated HNO_3. The resulting solutions were diluted using 5% (v/v) HNO_3 to produce 10 mL samples containing ~20 ppm U and K and ~3 ppm Li. These solutions were introduced into a PerkinElmer inductively coupled plasma optical emission spectrometer (ICP-OES) for chemical analysis.

C, H, and N Analysis. Crystals were isolated and rinsed with water and were analyzed using a Costech elemental analyzer (ECS 4010).

Thermogravimetric Analysis (TGA). About 15 mg of crystals for each compound was placed in an alumina crucible and heated using a Mettler Toledo thermal gravimetric analyzer from 25 to 900 °C at a rate of 5 °C/min under flowing air.

Powder X-ray Diffraction. The TGA residue of crystals after heating was used for measurement of powder X-ray diffractograms (PXRD) using a Bruker D8 ADVANCE diffractometer with DAVINCI design. The data were collected over a 2θ range from 5 to 55° with a step size of 0.02°. The count time for per step was 14 s.

Spectroscopic Characterization. Infrared spectra of single crystals for each compound were collected from 600 to 4000 cm^{-1} using a SensIR technology IlluminatIR FT-IR microspectrometer. This was done by placing crystals on a glass slide and crushing them with a diamond attenuated total reflectance (ATR) objective on the microscope.

Raman spectra for reaction solutions of compounds **1–4** and U_{60} harvested 3 days after the combination of solutions were collected using a Bruker Sentinel system linked via fiber optics to a Raman probe equipped with a 785 nm, 400 mW laser and a high-sensitivity, TE-cooled, 1024 × 255 CCD array. The spectra were collected for 15 s with three signal accumulations in the range from 80 to 3200 cm^{-1}. Raman spectra of crystals of each of the four compounds were collected as well using 5 s scans with 5 signal accumulations and the above-described spectrometer mounted on a microscope, together with a video-assisted fiber optic probe.

UV–vis spectra were collected for crystals of the four compounds using a Craig Instruments spectrometer from 250 to 1400 nm.

Small Angle X-ray Scattering. The mother solution of cluster U_{60} and the reaction solution of compound **4** were sealed in 0.5 mm diameter glass capillaries using wax. Water was sealed in an identical capillary for background measurement. Small angle X-ray scattering (SAXS) data were measured under a vacuum using a Bruker Nanostar equipped with a Cu microfocus source, Montel multilayer optics, and a

HiSTAR multiwire detector. The sample-to-detector distance was 26.3 cm, and the data collection time was 1 h.

■ RESULTS

Species in Reaction Solutions. In this study, the synthesis of compounds **1–3** was achieved by one-pot reactions using a combination of solutions including uranyl nitrate, hydrogen peroxide, H_2K_2EDTA, and other reagents. Compound **4** was produced using a two-step reaction of a solution of H_2K_2EDTA and the mother solution of cluster U_{60} that contained uranyl peroxide nanoclusters. Raman spectra (Figure 1) were used to
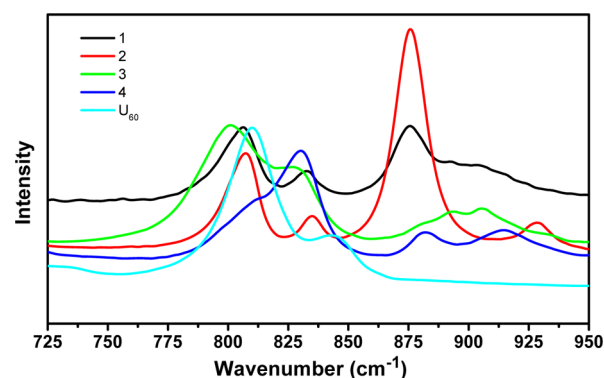

Figure 1. Raman spectra of reaction solutions of compounds **1–4** and mother solution of U_{60}.

probe the species in the reaction solutions of **1–4** and the mother solution of U_{60}. The UO_2^{2+} stretch mode was found at 806.5, 807.5, 800.5, 811.5, and 809.5 cm^{-1} for solutions corresponding to the syntheses of **1–4** and U_{60}, respectively.[8] The red shift of the UO_2^{2+} stretch for compound **3** is due to the partial overlap of vibrational modes for UO_2^{2+}, tetraethylammonium cations, and the IO_3^- group.[53] The O–O stretch of peroxide coordinated to uranyl was located at 832.9, 835.0, 828.5, 830.2, and 836.0 cm^{-1} for compounds **1–4** and U_{60}, respectively.[8] These results demonstrated formation of uranyl peroxide complexes in the reaction solutions and mother solution of U_{60}. As indicated by the SAXS data (Figure 2), the uranyl peroxide species in the mother solution of the cluster U_{60} have dimensions in the range of a few nanometers. However, these nanoclusters decomposed upon the addition of H_2K_2EDTA solution, likely due to the pH reduction.
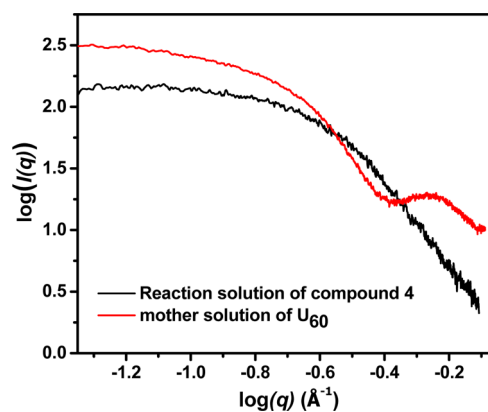

Figure 2. SAXS log–log plots for the mother solution of U_{60} and reaction solution of compound **4**.

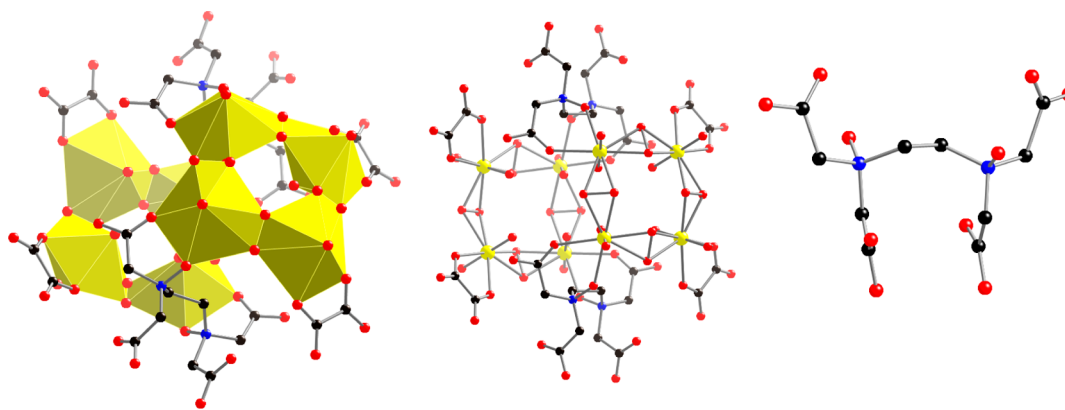**Figure 3.** Polyhedral (left) and ball−stick (middle) representations of the structure of compound **1** and a ball−stick representation of EDTAO$_2^{4-}$ (right). Uranyl polyhedra are shown in yellow, O atoms in red, N atoms in blue, and C atoms in black.
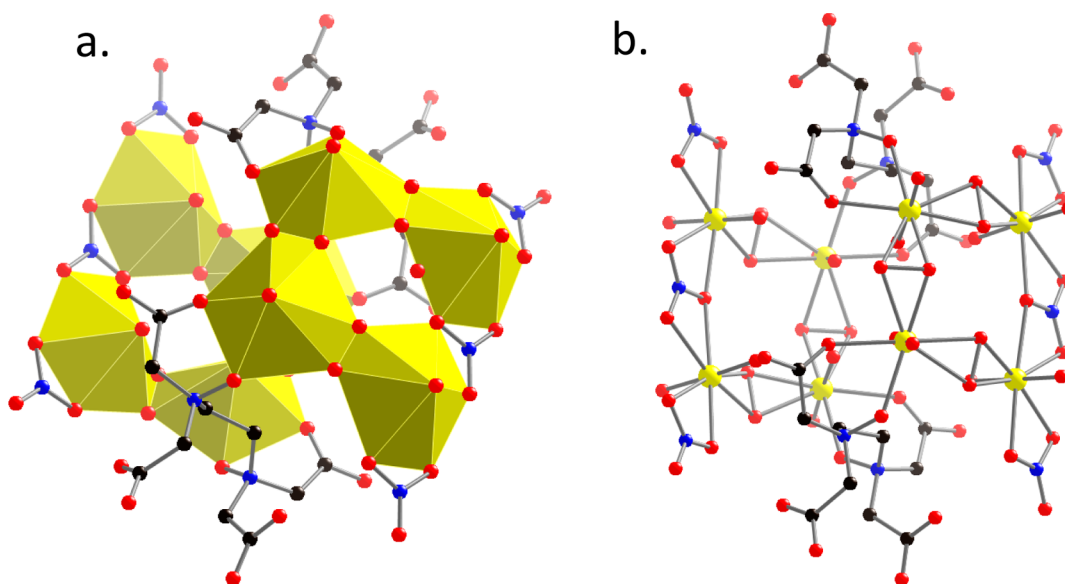

Figure 4. Polyhedral (a) and ball−stick (b) representations of the structure of compound **2**. Legend as in Figure 3.

For reaction solutions of compounds **1** and **2**, there are also Raman bands located at about 876 cm^{-1} that are assigned to the O−O stretch of free peroxide in solution,[54] demonstrating its presence in addition to the peroxide bound to uranyl ions. No such band was found in the spectrum of the reaction solution of compound **3**, although excess hydrogen peroxide was initially used in the one-pot reaction. This is attributed to the partial reduction of iodate by hydrogen peroxide that consumed the excess hydrogen peroxide in the solution by a Bray−Liebhafsky reaction that results in no solid I$_2$.[55] As demonstrated by the Raman spectrum, the mother solution of cluster U$_{60}$ lacks free peroxide, which is unstable in the alkaline reaction and decomposes with time.[56] As a result, the reaction solution of compound **4** also contained no free peroxide. Broad peaks centered at 882 cm^{-1} in the Raman spectra of compounds **3** and **4** are due to the stretch of C−C bonds in EDTA.[57] For compounds **1** and **2**, this band partially overlaps with that of free peroxide.

Structure Descriptions. X-ray diffraction data permitted the solution and refinement of the structures of four novel uranyl peroxide compounds containing EDTA molecules (Figures 3−6). In each of these the U(VI) cations are present as part of typical (UO$_2$)$^{2+}$ uranyl ions, with U≡O bond lengths at ~1.8 Å and O−U−O bond angles at ~180°. These uranyl ions are coordinated by various combinations of peroxo, EDTA, oxalate, nitrate, iodate, and/or H$_2$O groups, giving hexagonal bipyramidal coordination environments about the U(VI) cations, with the apexes of these bipyramids corresponding to the O atoms of the uranyl ions. Two distinct types of EDTA groups occur in these structures, one unoxidized and the other in which N atoms have been oxidized into −N−O groups. These two types of EDTA groups are hereafter designated as EDTA^{4-} (Figure 5c) and EDTAO$_2^{4-}$ (Figure 3c), respectively.

The structure of **1** contains tetramers of uranyl peroxide polyhedra in which the uranyl ions are bridged by bidentate peroxo groups, forming a ring structure (Figure 3). This unit is common in uranyl peroxide compounds, although it is typically one of the building units of uranyl peroxide cage clusters. Two such tetramers are linked together through two oxidized EDTAO$_2^{4-}$ ligands, resulting in novel octamers of uranyl hexagonal bipyramids.

Each uranyl ion in **1** is coordinated by two bidentate peroxo groups and two O atoms provided by either oxalate or EDTAO$_2^{4-}$ ligands, all of which are arranged at the equatorial vertices of hexagonal bipyramids. There are two crystallo-
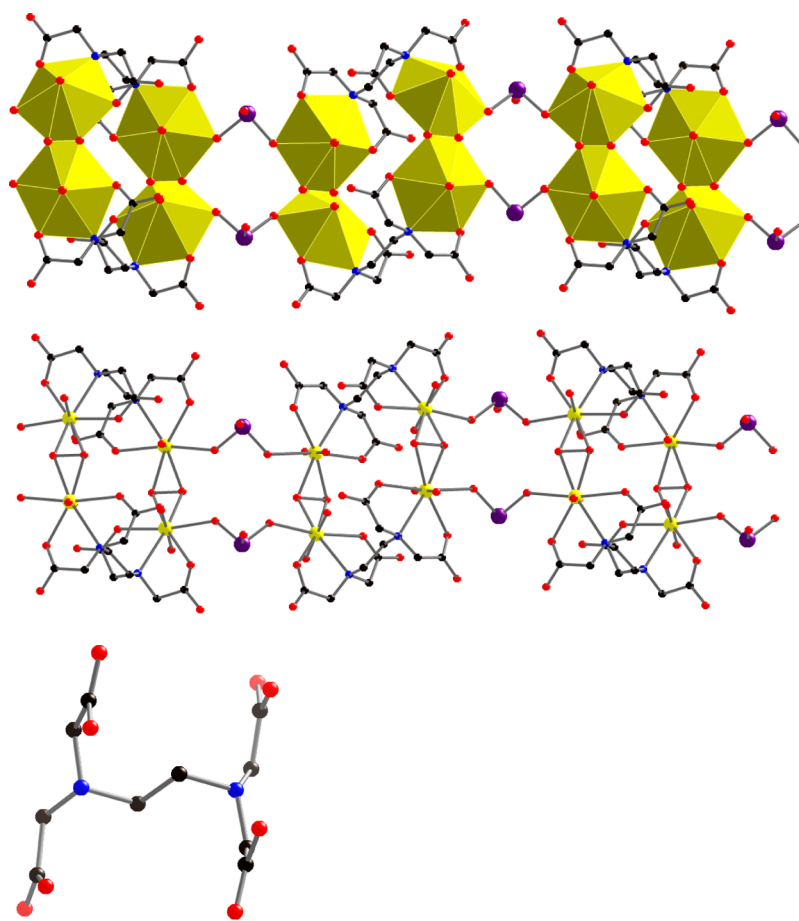
Figure 5. Polyhedral (top) and ball–stick (middle) representations of the structure of compound **3** and a ball–stick representation of EDTA^{4-} (bottom). Uranyl polyhedra are shown in yellow, O atoms in red, N atoms in blue, C atoms in black, and I atoms in purple.
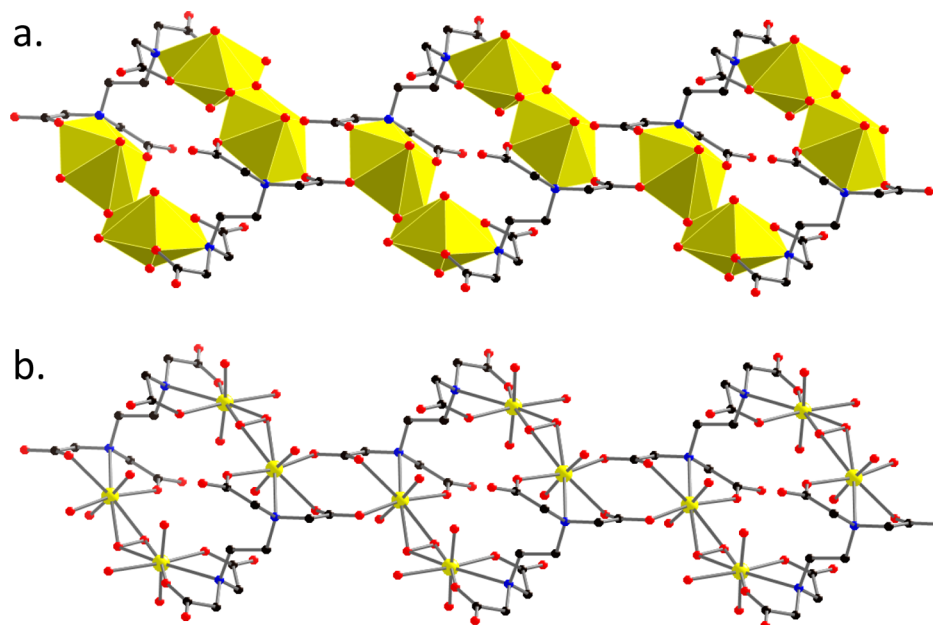

Figure 6. Polyhedral (a) and ball–stick (b) representations of the structure of compound **4**. Legend as in Figure 3.

graphically distinct uranyl ions, the coordination environment of one includes two O atoms from an oxalate group, whereas that of the other contains one O atom from a N–O group and one carboxylate O atom of the EDTAO$_2^{4-}$ ligand. The

EDTAO$_2^{4-}$ ligand acts as a tetradentate ligand in **1**: one carboxylate O atom and the O atom of a N–O group in one of the $-$NO(CH$_2$COO$^-$)$_2$ groups of EDTAO$_2^{4-}$ are coordinated to a uranyl ion in one tetramer, and two O atoms in the other

$-NO(CH_2COO^-)_2$ group are coordinated to a uranyl ion in the other tetramer of the octomer. The symmetry of the octamer is C_{2h}.

The structure of **2** contains a uranyl octamer consisting of two uranyl peroxide tetramers and two oxidized $EDTAO_2^{4-}$ ligands (Figure 4), as in **1**. However, the tetramer of uranyl ions in **2** contains only three peroxo bridges, rather than four as in **1**, and two of the uranyl polyhedra are bridged by the sharing of three vertices with a tridentate nitrate group. Four other nitrate groups act as bidentate ligands in **2**, and each shares one edge with a uranyl polyhedron. The symmetry of the octamer is C_{2h}.

The structure of **3** contains pairs of uranyl ions that are bridged by a bidentate peroxide group, resulting in a dimer of uranyl hexagonal bipyramids. Adjacent dimers are bridged by two hexadentate $EDTA^{4-}$ groups to form units containing four uranyl polyhedra, and these are further bridged by IO_3^- groups into infinite chains (Figure 5). Each uranyl ion in the dimer is coordinated by one O atom from an IO_3^- group, two peroxo O atoms, and one N atom as well as two carboxylate O atoms from one $-N(CH_2COO^-)_2$ group of an $EDTA^{4-}$ ligand, all of which are arranged at the equatorial vertices of the hexagonal bipyramid. The structure of compound **4** also consists of a one-dimensional unit that is formed by the linking of dimers of uranyl peroxide polyhedra through heptadentate $EDTA^{4-}$ ligands (Figure 6). Linkages between the uranyl ions and $EDTA^{4-}$ ligands are similar to those in **3** and result in a larger unit that contains four uranyl hexagonal bipyramids. In contrast to **3**, the seventh donor atom of the $EDTA^{4-}$ ligand, a carboxylate O atom, links the pairs of dimers of uranyl polyhedra into a chain, in a similar fashion to the IO_3^- group in **3**. Of the two crystallographically distinct uranyl ions in **4**, one is coordinated by one H_2O group, two peroxo O atoms, and one N atom as well as two carboxylate O atoms from one $-N(CH_2COO^-)_2$ group of an $EDTA^{4-}$ ligand. The other uranyl ion is coordinated by two peroxo O atoms, one N atom, as well as two carboxylate O atoms from one $-N(CH_2COO^-)_2$ group of an $EDTA^{4-}$ ligand, and one carboxylate O atom from a separate $EDTA^{4-}$ ligand.

Compounds **1**−**4** exhibit typical polyhedral geometries, with uranyl ion U≡O bond lengths ranging from 1.764(8) to 1.818(9) Å with a grand average of 1.793(13) Å, which is similar to the average of 1.783(30) from a variety of well-refined inorganic structures.[32] In each compound peroxide groups bridge uranyl ions, with the peroxide bidentate to the uranyl. The peroxide O−O bond lengths range from 1.464(16) to 1.522(12) Å, and the U−O_2−U dihedral angles range from 135.9 to 145.6°, which is the typical bent configuration for this unit.

The K, Na, and Li cations occur in typical and unremarkable coordination environments across compounds **1**−**4**. The iodate anion contains a stereoactive lone-pair that forces a trigonal pyramidal geometry with the bond lengths to oxygen ranging between 1.78(1) to 1.811(8) Å.

Spectroscopy. Raman spectra demonstrate the presence of UO_2^{2+}, peroxide, EDTA, and/or other ligands in compounds **1**−**4** (Figure 7). For **1**, the bands centered at 819 and 852 cm^{-1} are assigned as UO_2^{2+} and O−O stretching, respectively.[8] That at 884 cm^{-1} is due to the C−C stretch of the EDTA ligand.[58] For **2**, bands for UO_2^{2+} and O−O stretching appear at 817 and 843 cm^{-1}, respectively, and that due to NO_3 is at 1054 cm^{-1}.[59] For **3**, bands arising from IO_3^- and UO_2^{2+} stretching partially overlap at ∼790 cm^{-1},[53] the peroxide stretch is at 835 cm^{-1},[8] and the C−C stretch of EDTA is at 885 cm^{-1}.[58] The weak band
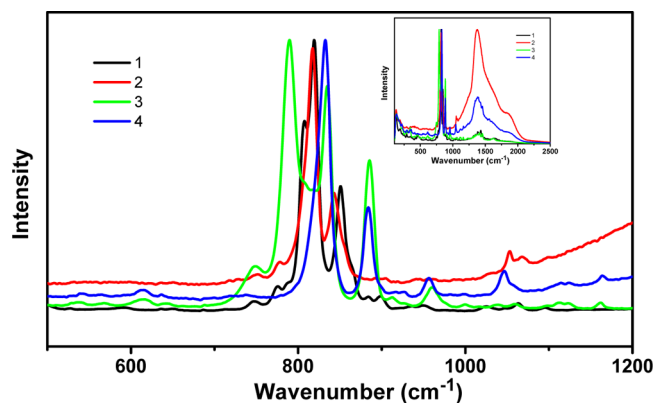

Figure 7. 500−1200 cm^{-1} region of the Raman spectra of compounds **1**−**4**. The inset is a broader spectral range.

at 614 cm^{-1} is assigned to the UO_2^{2+}−N stretch.[60] For **4**, bands for uranyl and peroxide partially overlap at 833 cm^{-1}, and the C−C stretch of EDTA is at 884 cm^{-1}.[58] There is also a weak band at 614 cm^{-1} due to UO_2^{2+}−N bond stretching.[60]

IR spectra of **1**−**4** displayed similar features (Figure 8). Bands centered at about 871, 879, 890, and 890 cm^{-1} for
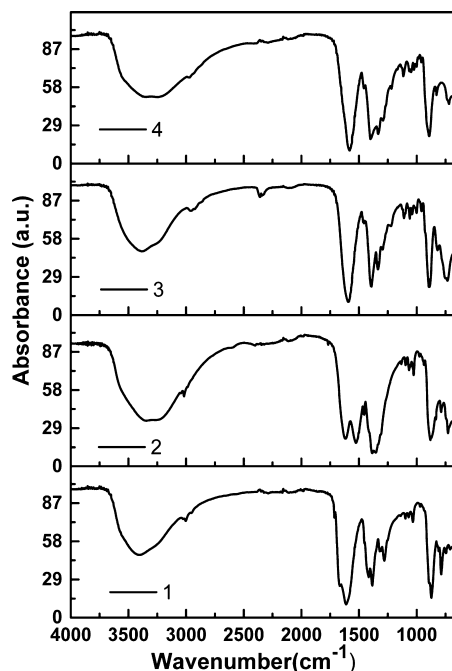

Figure 8. IR spectra of compounds **1**−**4**.

compounds **1**−**4**, respectively, are assigned to UO_2^{2+} stretching.[61,62] Weak bands in the range of 1000 to 1100 cm^{-1} may correspond to C−C and C−N stretches of EDTA.[63] The broad and strong bands centered at about 1613, 1617, 1594, and 1585 cm^{-1} for **1**−**4** are asymmetric stretching frequency of the carboxylate group of EDTA.[63] Broad bands in the region from about 2600 to 3600 cm^{-1} are due to H bonds. The symmetric stretching mode of the NO_3^- group occurs at about 1026 cm^{-1} for **2**,[61] and the IO_3^- mode occurs at 750 cm^{-1} for **3**.[62,64]

UV−vis spectra of **1**−**4** displayed similar features and demonstrate the presence of uranyl ions in each compound (Figure S1).

Composition. The X-ray crystallographic analysis provided the formula $[NaK_{15}[(UO_2)_8(O_2)_8(C_{10}H_{12}O_{10}N_2)_2(C_2O_4)_4]\cdot(H_2O)_{14}]$ for **1**. Refinement of the K site occupancies indicates some of them are partially vacant (summing to 14.2), presumably owing to charge-balance requirements. The assigned formula of compound **2** is $[Li_4K_6[(UO_2)_8(O_2)_6(C_{10}H_{12}O_{10}N_2)_2(NO_3)_6]\cdot(H_2O)_{26}]$, which includes partial occupancies of the K sites as revealed by the structure refinement, and assumes partial occupancies of the Li sites to achieve charge balance.

For **3**, the X-ray crystallographic analysis, chemical analysis, and TGA revealed the formula $[K_4[(UO_2)_4(O_2)_2(C_{10}H_{13}O_8N_2)_2(IO_3)_2]\cdot(H_2O)_{16}]$. ICP-OES analysis confirmed the atomic ratio of U/K = 1:1. Crystals of **3** were measured using a CHN analyzer to confirm C, H, and N. Anal. Calcd for the complex $C_{20}N_4H_{58}O_{50}K_4U_4I_2$: C, 9.5; H, 2.3; N, 2.2. Found: C, 9.1; H, 2.0; N, 2.1. The pK_a for EDTA are $pK_{a1} = 0$, $pK_{a2} = 1.5$, $pK_{a3} = 2.0$, $pK_{a4} = 2.66$, $pK_{a5} = 6.16$, and $pK_{a6} = 10.24$. The first four pK_a values correspond to the COOH protons, and the other two are for the two NH^+ protons. Compound **3** formed in a weak acid solution, and therefore EDTA is likely to be partly protonated, as assumed in the structural formula to provide charge balance. Thermogravimetric analysis (TGA) of crystals of **3** indicated a 47% weight loss (Figure S2, Supporting Information). The powder X-ray diffraction pattern (Figure S3, Supporting Information) of the TGA residue identified it as $K_2U_2O_7$. Sixteen H_2O groups per formula unit are consistent with the TGA analysis and the crystal structure determination.

For **4**, the X-ray crystallographic analysis combined with the chemical data indicate the formula $LiK_3[(UO_2)_4(O_2)_2(C_{10}H_{12}O_8N_2)_2(H_2O)_2]\cdot(H_2O)_{18}$. The Li was not located in the X-ray structure, where it may be disordered or masked by its low X-ray scattering efficiency, but ICP-OES analysis provided the atomic ratios U/K/Li = 4:3:0.8. TGA analysis (Figure S2) confirmed 18 H_2O per formula unit. Crystals of **4** were measured using a CHN analyzer: Anal. Calcd for the complex $C_{20}N_4H_{64}O_{48}Li_1K_3U_4$: C, 10.9; H, 2.9; N, 2.5. Found: C, 10.2; H, 2.0; N, 2.9.

DISCUSSION

The most interesting aspect of uranyl peroxide chemistry is arguably the strong tendency for assembly of cage clusters. Experimental and computational studies indicate that an inherently bent $U-O_2-U$ dihedral angle encourages the curvature necessary for cage-cluster formation.[22,23] All structures published to date that contain uranyl ions bridged through peroxide exhibit bent $U-O_2-U$ interactions, but many of these occur in cage clusters, and it could be argued that steric constraints require the bent $U-O_2-U$ configuration. Compounds **1**–**4** contain uranyl peroxide building units that also occur in larger cage clusters, without the associated steric constraints in this case. As in all other structures with the $U-O_2-U$ bridge, the dihedral angle is strongly bent at ~140°.

Although the cage-forming tendency is very strong in aqueous uranyl peroxide solutions, the current study demonstrates that introduction of multidentate EDTA groups interrupts the cooperative connection of bent $U-O_2-U$ bridges to form cage clusters and instead results in compounds with smaller uranyl peroxide units. Compound **4** formed when H_2K_2EDTA was added to a solution that contained U_{60}, the breakdown of which may have been favored by the reduction in pH due to the addition of H_2K_2EDTA. Overall, the oxalate, nitrate, iodate, and EDTA that coordinate the uranyl ions in

these compounds interrupts the cage-cluster-forming tendency of uranyl peroxide polyhedra. Although the typical bent $U-O_2-U$ configuration persists in these structures, incorporation of additional anions favors fewer peroxide bridges between uranyl ions, resulting in simpler uranyl peroxide units.

Excess peroxide existed in reaction solutions that produced **1** and **2**, as shown by Raman spectroscopy, and $EDTA^{4-}$ was oxidized to $EDTAO_2^{4-}$. Reactions between iodate and peroxide apparently consumed the excess peroxide in the reaction solution of compound **3**, the $EDTA^{4-}$ was not oxidized, and it was incorporated into **3**. The synthesis of compound **4** contained no excess peroxide, and unoxidized $EDTA^{4-}$ was incorporated in the crystals.

The oxidized $EDTAO_2^{4-}$ ligand in compounds **1** and **2** is bidentate to each uranyl ion, and the $EDTA^{4-}$ ligand in compounds **3** and **4** is tridentate to each uranyl ion. As such, uranyl ions in **1** and **2** can be coordinated by two bidentate peroxide groups, which is essential for the formation of the uranyl peroxide tetramers. However, each uranyl ion in compounds **3** and **4** can only be coordinated by one bidentate peroxide, limiting the role of peroxide bridges to that of producing dimers of uranyl polyhedra only. Oxidation of N atoms and formation of $-N-O$ groups in EDTA impact its coordination mode, and this influences the topology of the uranyl peroxide structural unit.

CONCLUSIONS

Herein, we report the synthesis and structures of the first four uranyl peroxide compounds containing EDTA by controlling the amount of peroxide in reaction solutions with a pH range of 5−7. Excess peroxide in solution has oxidized the $EDTA^{4-}$ to $EDTAO_2^{4-}$ in two cases. Structures of the four compounds demonstrate that $EDTA^{4-}$ and $EDTAO_2^{4-}$ had different coordination modes for uranyl ions that impact the final topology of the uranyl peroxide structures. Structures of compounds **1** and **2** isolated from solutions with excess peroxide contain octamers of uranyl polyhedra with $EDTAO_2^{4-}$, whereas structures of compounds **3** and **4** isolated from solutions without free peroxide are based on infinite chains and unoxidized $EDTA^{4-}$.

ASSOCIATED CONTENT

ⓢ Supporting Information

X-ray crystallographic file in CIF format for compounds **1**−**4**, UV−vis spectra of compounds **1**−**4**, thermograms of compounds **3** and **4**, and PXRD patterns of TGA residues of compounds **3** and **4**. This material is available free of charge via the Internet at http://pubs.acs.org.

AUTHOR INFORMATION

Corresponding Author

*E-mail: pburns@nd.edu.

Notes

The authors declare no competing financial interest.

ACKNOWLEDGMENTS

■ REFERENCES

(1) Odoh, S. O.; Schreckenbach, G. *Inorg. Chem.* **2013**, *52*, 5590−5602.

(2) Wylie, E. M.; Peruski, K. M.; Weidman, J. L.; Phillip, W. A.; Burns, P. C. *ACS Appl. Mater. Interfaces* **2014**, *6*, 473−479.

(3) Kubatko, K. A. H.; Helean, K. B.; Navrotsky, A.; Burns, P. C. *Science* **2003**, *302*, 1191−1193.

(4) McNamara, B.; Buck, E.; Hanson, B. In *Scientific Basis for Nuclear Waste Management XXVI*; 2002 MRS Fall Meeting - Symposium II; Finch, R. J., Bullen, D. B., Eds.; Materials Research Society: Warrendale, PA , 2003; Vol. 757, p 401−406.

(5) Burakov, B. E.; Strykanova, E. E.; Anderson, E. B. In *Scientific Basis for Nuclear Waste Management XX*; Symposium held December 2−6, 1996, Boston, Massachusetts, USA; Gray, W. J., Triay, I. R., Eds.; Materials Research Society: Warrendale, PA , 1997; Vol. *465*, pp 1309−1311.

(6) Burns, P. C.; Hughes, K. A. *Am. Mineral.* **2003**, *88*, 1165−1168.

(7) Amme, M.; Renker, B.; Schmid, B.; Feth, M. P.; Bertagnolli, H.; Dobelin, W. *J. Nucl. Mater.* **2002**, *306*, 202−212.

(8) Bastians, S.; Crump, G.; Griffith, W. P.; Withnall, R. *J. Raman Spectrosc.* **2004**, *35*, 726−731.

(9) Clarens, F.; De Pablo, J.; Diez-Perez, I.; Casas, I.; Gimenez, J.; Rovira, M. *Environ. Sci. Technol.* **2004**, *38*, 6656−6661.

(10) Mallon, C.; Walshe, A.; Forster, R. J.; Keyes, T. E.; Baker, R. J. *Inorg. Chem.* **2012**, *51*, 8509−8515.

(11) Rey, A.; Utsunomiya, S.; Gimenez, J.; Casas, I.; de Pablo, J.; Ewing, R. C. *Am. Mineral.* **2009**, *94*, 229−235.

(12) Gimenez, J.; Martinez-Llado, X.; Rovira, M.; de Pablo, J.; Casas, I.; Sureda, R.; Martinez-Esparza, A. *Radiochim. Acta* **2010**, *98*, 479−483.

(13) Sureda, R.; Martinez-Llado, X.; Rovira, M.; de Pablo, J.; Casas, I.; Gimenez, J. *J. Hazard. Mater.* **2010**, *181*, 881−885.

(14) Douglas, M.; Clark, S. B.; Friese, J. I.; Arey, B. W.; Buck, E. C.; Hanson, B. D. *Environ. Sci. Technol.* **2005**, *39*, 4117−4124.

(15) Qiu, J.; Burns, P. C. *Chem. Rev.* **2013**, *113*, 1097−1120.

(16) Qiu, J.; Kevin, N.; Jouffret, L.; Szymanowski, J. E. S.; Burns, P. C. *Inorg. Chem.* **2013**, *52*, 337−345.

(17) Qiu, J.; Ling, J.; Jouffret, L.; Thomas, R.; Szymanowski, J. E. S.; Burns, P. C. *Chem. Sci.* **2014**, *5*, 303−310.

(18) Burns, P. C. *Mineral. Mag.* **2011**, *75*, 1−25.

(19) Thuery, P.; Masci, B. *Supramol. Chem.* **2003**, *15*, 95−99.

(20) Burns, P. C.; Kubatko, K. A.; Sigmon, G.; Fryer, B. J.; Gagnon, J. E.; Antonio, M. R.; Soderholm, L. *Angew. Chem., Int. Ed.* **2005**, *44*, 2135−2139.

(21) Armstrong, C. R.; Nyman, M.; Shvareva, T.; Sigmon, G. E.; Burns, P. C.; Navrotsky, A. *Proc. Natl. Acad. Sci. U. S. A.* **2012**, *109*, 1874−1877.

(22) Sigmon, G. E.; Ling, J.; Unruh, D. K.; Moore-Shay, L.; Ward, M.; Weaver, B.; Burns, P. C. *J. Am. Chem. Soc.* **2009**, *131*, 16648−16649.

(23) Vlaisavljevich, B.; Gagliardi, L.; Burns, P. C. *J. Am. Chem. Soc.* **2010**, *132*, 14503−14508.

(24) Kubatko, K.-A.; Burns, P. C. *Inorg. Chem.* **2006**, *45*, 6096−6098.

(25) Alcock, N. W. *J. Chem. Soc. A* **1968**, 1588−1594.

(26) Zehnder, R. A.; Peper, S. M.; Scott, B. L.; Runde, W. H. *Acta Crystallogr. Sect. C: Cryst. Struct. Commun.* **2005**, *61*, I3−I5.

(27) Kubatko, K.-A.; Forbes, T. Z.; Klingensmith, A. L.; Burns, P. C. *Inorg. Chem.* **2007**, *46*, 3657−3662.

(28) Zehnder, R. A.; Batista, E. R.; Scott, B. L.; Peper, S. M.; Goff, G. S.; Runde, W. H. *Radiochim. Acta* **2008**, *96*, 575−578.

(29) Nyman, M.; Rodriguez, M. A.; Campana, C. F. *Inorg. Chem.* **2010**, *49*, 7748−7755.

(30) Masci, B.; Thuery, P. *Polyhedron* **2005**, *24*, 229−237.

(31) Unruh, D. K.; Burtner, A.; Burns, P. C. *Inorg. Chem.* **2009**, *48*, 2346−2348.

(32) Burns, P. C. *Can. Mineral.* **2005**, *43*, 1839−1894.

(33) Nowack, B.; VanBriesen Jeanne, M. In *Biogeochemistry of Chelating Agents*; American Chemical Society: Washington, DC, 2005; Vol. *910*, pp 1−18.

(34) Serne, R. J.; Cantrell, C. J.; Lindenmeier, C. W.; Owen, A. T.; Kutnyakov, I. V.; Orr, R. D.; Felmy, A. R.*Radionuclide-Chelating Agent Complexes in Low-Level Radioactive Decontamination Waste; Stability, Adsorption and Transport Potential*; PNNL-13774; Pacific Northwest National Laboratory, U.S. Nuclear Regulatory Commission, Office of Nuclear Research, Washington, DC, 2002

(35) Read, D.; Ross, D.; Sims, R. J. *J. Contamin. Hydrol.* **1998**, *35*, 235−248.

(36) Barger, M.; Koretsky, C. M. *Appl. Geochem.* **2011**, *26*, S158−S161.

(37) Suzuki, Y.; Tanaka, K.; Kozai, N.; Ohnuki, T. *Geomicrobiol. J.* **2010**, *27*, 245−250.

(38) Haas, J. R.; Northup, A. *Geochem. Trans.* **2004**, *5*, 41−48.

(39) Shchelokov, R. N.; Orlova, I. M.; Sergeev, A. V.; Mikhailov, Y. N.; Lobanova, G. M.; Kanishcheva, A. S. *Koord. Khim.* **1985**, *11*, 196−206.

(40) Mikhailov, Y. N.; Lobanova, G. M.; Kanishcheva, A. S.; Sergeev, A. V.; Bolotova, G. T.; Shchelokov, R. N. *Koord. Khim.* **1985**, *11*, 545−550.

(41) Weakliem, H. A.; Hoard, J. L. *J. Am. Chem. Soc.* **1959**, *81*, 549−555.

(42) Bayot, D.; Tinant, B.; Mathieu, B.; Declercq, J. P.; Devillers, M. *Eur. J. Inorg. Chem.* **2003**, 737−743.

(43) Bayot, D.; Tinant, B.; Devillers, M. *Inorg. Chem.* **2004**, *43*, 5999−6005.

(44) Kaplun, M.; Sandstrom, M.; Bostrom, D.; Shchukarev, A.; Persson, P. *Inorg. Chim. Acta* **2005**, *358*, 527−534.

(45) Wang, C. C.; Yang, C. H.; Lee, C. H.; Lee, G. H. *Inorg. Chem.* **2002**, *41*, 429−432.

(46) Shi, Z.; Feng, S. H.; Sun, Y.; Hua, J. *Inorg. Chem.* **2001**, *40*, 5312−5313.

(47) Hu, S.; Sheng, T.; Wen, Y.; Fu, R.; Wu, X. *Inorg. Chem. Commun.* **2012**, *16*, 28−32.

(48) Liu, D.-S.; Sui, Y.; Li, C.-H.; Cheng, W.-T.; Wang, T.-W.; You, X.-Z. *Inorg. Chim. Acta* **2011**, *376*, 112−117.

(49) Stavila, V.; Gulea, A.; Popa, N.; Shova, S.; Merbach, A.; Simonov, Y. A.; Lipkowski, J. *Inorg. Chem. Commun.* **2004**, *7*, 634−637.

(50) Sigmon, G. E.; Unruh, D. K.; Ling, J.; Weaver, B.; Ward, M.; Pressprich, L.; Simonetti, A.; Burns, P. C. *Angew. Chem., Int. Ed.* **2009**, *48*, 2737−2740.

(51) Sheldrick, G. M. *SADABS-Bruker AXS Area Detector Scaling and Adsorption*, version 2008/1; University of Gottingen: Germany, 2008.

(52) Sheldrick, G. M. *Acta Crystallogr. Sect. A: Found. Crystallogr.* **2008**, *64*, 112−122.

(53) Durig, J. R.; Bonner, O. D.; Breazeal, W. *J. Phys. Chem.* **1965**, *69*, 3886−3892.

(54) Venkateswaran, S. *Nature* **1931**, *127*, 406−406.

(55) Schmitz, G.; Furrow, S. *Phys. Chem. Chem. Phys.* **2012**, *14*, 5711−5717.

(56) Nicoll, W. D.; Smith, A. F. *Ind. Eng. Chem.* **1955**, *47*, 2548−2554.

(57) Nuttall, R. H.; Stalker, D. M. *Inorg. Nucl. Chem. Lett.* **1976**, *12*, 639−641.

(58) Krishnan, K.; Plane, R. A. *J. Am. Chem. Soc.* **1968**, *90*, 3195−3200.

(59) Brooker, M. H.; Huang, C. H.; Sylwestrowicz, J. *J. Inorg. Nucl. Chem.* **1980**, *42*, 1431−1440.

(60) Bradley, D. C.; Gitlitz, M. H. *Nature* **1968**, *218*, 353−354.

(61) Bullock, J. I. *J. Inorg. Nucl. Chem.* **1967**, *29*, 2257−2264.

(62) Ling, J.; Albrecht-Schmitt, T. E. *Inorg. Chem.* **2007**, *46*, 346−347.

(63) Faulques, E.; Perry, D. L.; Lott, S.; Zubkowski, J. D.; Valente, E. J. *Spectrochim. Acta A Mol. Biomol. Spectrosc.* **1998**, *54*, 869−878.

(64) Sykora, R. E.; McDaniel, S. M.; Wells, D. M.; Albrecht-Schmitt, T. E. *Inorg. Chem.* **2002**, *41*, 5126−5132.